C.P. No. 893

C.P. No. 893

MINISTRY OF AVIATION

AERONAUTICAL RESEARCH COUNCIL

CURRENT PAPERS

The Performance of Conical Convergent-Divergent Nozzles of Area Ratio 2.44 and 2.14 in External Flow

By

G. T. Golesworthy

J. B. Roberts and C. Overy

LONDON: HER MAJESTY'S STATIONERY OFFICE

1966

SIX SHILLINGS NET

U.D.C. No. 621-225.1:533.691.18

C.P. No.893*

o

The performance of conical convergent-divergent nozzles of area ratios 2.44 and 2.14 in external flow

- by -

G. T. Golesworthy, J. B. Roberts and C. Overy

SUMMARY

Two model internal-expansion propelling nozzles with conical divergence of 10° semi-angle, area ratios 2.44 and 2.14 (design pressure ratios 15 and 12), parallel afterbodies and thin annular bases, have been tested in external flow over the range of Mach No. 0.7 to 2.25. Measurements have been made of nozzle base pressure, and thrust efficiencies derived with reference to both ambient and base pressure levels.

It is found that, in supersonic external flow, with complete expansion of nozzle internal flow to ambient pressure, the value of base pressure ratio is independent of nozzle design pressure ratio, provided the base thickness is unchanged. For a given overall operating pressure ratio, again with constant base thickness, the effect of decreasing nozzle design pressure ratio is to raise base pressure ratio. In subsonic external flow, for a given overall operating pressure ratio, base pressure ratio can be independent of nozzle design pressure ratio.

---

*Replaces N.G.T.E. M.372 - A.R.C.26 494

CONTENTS

APPENDIX

Title

ILLUSTRATIONS

1.0 Introduction

In Reference 1 are described tests of an axisymmetric model internal-expansion propelling nozzle with area ratio 2.9 (design pressure ratio 20). The present work is concerned with two similar models with design pressure ratios of 12 and 15. These also have been tested in external flow over the range of Mach No. 0.7 to 2.25.

2.0 Test equipment

A description of the external flow rig usod for these tests will be found in Reference 1. Figure 1 illustrates the rig layout. It had two alternative working sections: a transonic giving external Mach numbers from 0.7 to 1.5, and a supersonic covering the range between 1.3 and 2.4. Test models were carried on a long parallel hollow sting, which could be arranged to pass through the throat of either external flow nozzle.

The two models, shown in Figures 2 and 3, utilised the same conical inlet and outlet sections as the model of Reference 1, new throat sections being fitted. Throat diameters were 2.180 and 2.327 in., giving ratios of plane outlet area/geometric throat area equal to 2.440 and 2.143 respectively. Approach and divergent semi-angles were 10°, and the radius of curvature of the throat transition was made equal to the throat radius in either case. As with the previous model, the afterbody continued parallel up to the outlet plane, forming an annular base 0.050 in. wide.

3.0 Instrumentation and air supplies

No thrust measuring equipment was fitted in this test rig, and model internal gross thrust was derived from:-

(i) Knowledge of discharge coefficient (C_D). This was taken to be 0.991 when choked, as for the model of Reference 1 with geometrically similar throat≠.

(ii) Calculated stream thrust at the throat plane.

(iii) Measurement of pressures along the divergent portion of the nozzle.

(iv) Measurement of base pressure.

(v) Computed allowance for friction.

The expression for gross thrust efficiency* was derived in Reference 2:-

$$\eta_F = \frac{1.2679\ C_D.\mu + \int_1^{A_e/A_g} \frac{P_w}{P_t}\, d\left(\frac{A}{A_g}\right) - \frac{1}{R}\cdot\frac{A_e}{A_g} - \phi}{0.012316\ C_D \left[\frac{v}{\sqrt{T_t}}\right]_R}$$

≠ Radius of throat curvature = ½ throat diameter

* For definition see Appendix

taking $\gamma = 1.4$,

where μ = vacuum stream thrust efficiency at the throat, taken to be 1.003 when choked as in References 1 and 4 for similar throat geometry.

In accordance with the argument presented in Reference 2, no correction for "real air" effects has been applied.

Pressure instrumentation on the models accordingly consisted of:-

(i) A rake of 7 pitot tubes 1 mm o.d. at entry, spaced on an equal-area basis.

(ii) Nine or eight static tappings spirally positioned down the divergent section, each 0.020 in. diameter.

(iii) Two tappings spaced 90° apart in the base annulus.

(iv) Two static tappings on the external surface.

External flow lines were fitted with wall pressure tappings, and these were considered to be more reliable in assessment of external Mach number than the model afterbody tappings.

Air supply temperature to both model and both the working sections were maintained within the range 25 to 35°C at all times, and no further attention was paid to temperature measurement. Air dryness was measured by an R.A.E.-Bedford pattern frost-point hygrometer, and held at better than -20°C throughout.

Supply pressure was at a level of 5 atmospheres, and throttled independently as required for model and external flow lines.

4.0 Model operating conditions

The following values of external Mach number were chosen:-

(i) Supersonic line: M_{∞} = 1.5, 1.75, 2.0, 2.25

(ii) Transonic line: M_{∞} = 0.7, 0.9, 1.1, 1.3, 1.5

At each Mach number the model was tested over a representative band of exhaust pressure ratio (E.P.R.) between the limits 2 and 20.

5.0 Model performance

5.1 Base pressure

As explained in Reference 1, the outer boundary layer at the end of the afterbody in these tests was somewhat thicker than would be representative of a typical flight installation. For this reason, base pressures in practice would tend to be rather lower than those measured here.

Two ways of presenting the base pressure information have been used. Figures 4 and 5 give the ratio $\frac{P_b}{P_\infty}\left(= \frac{E.P.R.}{A.P.R.}\right)^{\dagger}$, while Figures 6 and 7 show the base pressure coefficient, in both cases as functions of E.P.R. and M_∞. It will be observed that the value of $\frac{P_b}{P_\infty}$ drops fairly sharply at conditions of low E.P.R. and low M_∞, implying a quite large change in A.P.R. for a small variation in E.P.R. This same type of pattern was noted in Reference 1. In the present models (especially that with D.P.R.12)† this fall in $\frac{P_b}{P_\infty}$ is more limited in extent than was the case with D.P.R.20, and with further increase of E.P.R. (above 4) the base pressure ratio now rises again quite steeply. The higher Mach number curves lie close together in a band rising with E.P.R.

When completely expanded to ambient pressure (E.P.R. = D.P.R.) in supersonic external flow, both models give similar values of $\frac{P_b}{P_\infty}$. The additional evidence of Reference 1 suggests that for this condition, and with constant base thickness, the base pressure ratio is independent of D.P.R., the appropriate values for all three models lying in the band 0.62 to 0.68 according to external Mach number. This implies that all pressures within the base flow system can remain similar, although the nozzle outlet Mach number is changing. Such a conclusion is in line with theoretical work on backward-facing steps (e.g. Reference 5), which indicates that, providing all other quantities are maintained constant, variation of approach stream Mach number within similar limits has little effect on base pressure.

Information from References 1 and 3 has been incorporated in Figures 8 and 9, illustrating the behaviour of a number of conical convergent-divergent nozzles with the same divergence angle when immersed in subsonic and supersonic external flow. All models had parallel afterbodies of the same outside diameter, and variation of D.P.R. was achieved in two ways: in Reference 1 and the present work, by varying throat diameter and keeping base thickness fixed; in Reference 3 by fixing the throat diameter and varying base thickness.

Base pressure ratio in subsonic external flow is apparently unaffected by all geometric variables, as shown in Figure 8, so long as the E.P.R. is below the critical value at which $\frac{P_b}{P_\infty}$ turns sharply downwards (see Figures 4 and 5). In supersonic external flow (Figure 9) two effects can be distinguished for any fixed E.P.R. First, as D.P.R. is reduced with constant base thickness, the outlet flow becomes increasingly under-expanded, and $\frac{P_b}{P_\infty}$ rises. Secondly, for constant internal expansion (or D.P.R.), increase of base thickness lowers the value of $\frac{P_b}{P_\infty}$.

† For definitions see Appendix

Apparently, for the tests reported in Reference 3, these opposing effects have more or less cancelled out, and the results show very little influence of D.P.R.

5.2 Internal pressures

Typical pressure distributions are shown in Figures 10 and 11 for each model over a range of A.P.R. These were obtained in the transonic working section, where model entry conditions were such that a turbulent internal boundary layer would be expected. The separation pressure patterns correspond to this state. In the supersonic working section, very few instances of internal separation were encountered during these tests.

5.3 Thrust efficiency

Figures 12 and 13 give the nozzle thrust efficiency based on E.P.R. for each model, according to the relation in Section 3.0. Constant values of the friction correction term have been applied to each nozzle, namely 0.60 and 0.55 per cent for D.P.R.15 and 12 respectively. These values were obtained from the curves presented in Reference 4, taking the design-point operating conditions.

The same allowance for friction was made in the case of efficiency based on A.P.R., shown in Figures 14 and 15. Design-point efficiency levels came out as 0.995 and 0.9945 for D.P.R.15 and 12 respectively. It is thought that these values are about 0.5 per cent too high, and accuracy better than this would not be claimed for pressure plotting methods.

Finally, in Figures 16 and 17 is shown the quantity $\Delta\eta$, representing the deduction from $\eta_{F(EPR)}$ which is required to include the drag force on the annular base, according to the method of Reference 1.

6.0 Conclusion

The present work has extended that of Reference 1 to cover a family of three conical convergent-divergent model propelling nozzles with similar internal form, the same base thickness, and design pressure ratios of 20, 15 and 12.

When completely expanded to ambient pressure in supersonic external flow, all three nozzles produce similar values of base pressure ratio $\left(\frac{P_b}{P_\infty}\right)$, in the band 0.62 to 0.68 according to external Mach number. Also with supersonic external flow, but at constant exhaust pressure ratio $\left(\frac{P_t}{P_\infty}\right)$, the value of base pressure ratio for these nozzles rises with decrease in design pressure ratio, that is as the outlet flow becomes increasingly under-expanded. In subsonic external flow with representative exhaust pressure ratios, the base pressure ratio is effectively independent of nozzle design pressure ratio.

ACKNOWLEDGEMENT

The authors are indebted to Miss M. Faiers and Miss V. Searle for their assistance in this programme of tests.

REFERENCES

No.	Author(s)	Title, etc.
1	G. T. Golesworthy M. V. Herbert	The performance of a conical convergent-divergent nozzle with area ratio 2·9 in external flow. A.R.C. C.P. No.891 November, 1963
2	R. J. Herd G. T. Golesworthy	The performance of a centrebody propelling nozzle with a parallel shroud in external flow - Part I. A.R.C. C.P. No.841 November, 1963
3	J. B. Roberts G. T. Golesworthy	An experimental investigation of the influence of base bleed on the base drag of various propelling nozzle configurations. A.R.C. C.P. No.892 February, 1964
4	M. V. Herbert D. L. Martlew	The design-point performance of model internal-expansion propelling nozzles with area ratios up to 4. A.R.C. R. & M.3477 December, 1963
5	J. F. Nash	An analysis of two-dimensional turbulent base flow, including the effect of the approaching boundary layer. A.R.C. R. & M.3344 July, 1962

APPENDIX

Symbols and definitions

A^*	isentropic throat area
A_g	geometric throat area
A_e	geometric plane outlet area
C_D	discharge coefficient $= \dfrac{\text{actual air mass flow}}{\text{isentropic air mass flow for the same throat area}} = \dfrac{A^*}{A_g}$
M_∞	free-stream Mach number
P_t	model entry total pressure
P_b	model base pressure
P_w	model internal wall pressure
P_∞	free-stream static pressure
R	pressure ratio (see A.P.R. and E.P.R.)
Re*	model throat Reynolds number (based on throat diameter and sonic conditions)
T_t	model entry total temperature
v	isentropic velocity
η_F	gross thrust efficiency $\dfrac{\text{measured gauge thrust at given pressure ratio R}}{\text{gauge thrust of an isentropic nozzle, passing the same flow, at the same pressure ratio R, and fully expanded}}$
μ	vacuum stream thrust efficiency at the throat
ϕ	friction correction term
A.P.R.	applied pressure ratio $= \dfrac{\text{model entry total pressure}}{\text{model base pressure}} = \dfrac{P_t}{P_b}$
E.P.R.	exhaust pressure ratio $= \dfrac{\text{model entry total pressure}}{\text{free-stream static pressure}} = \dfrac{P_t}{P_\infty}$
D.P.R.	design pressure ratio

FIG. I

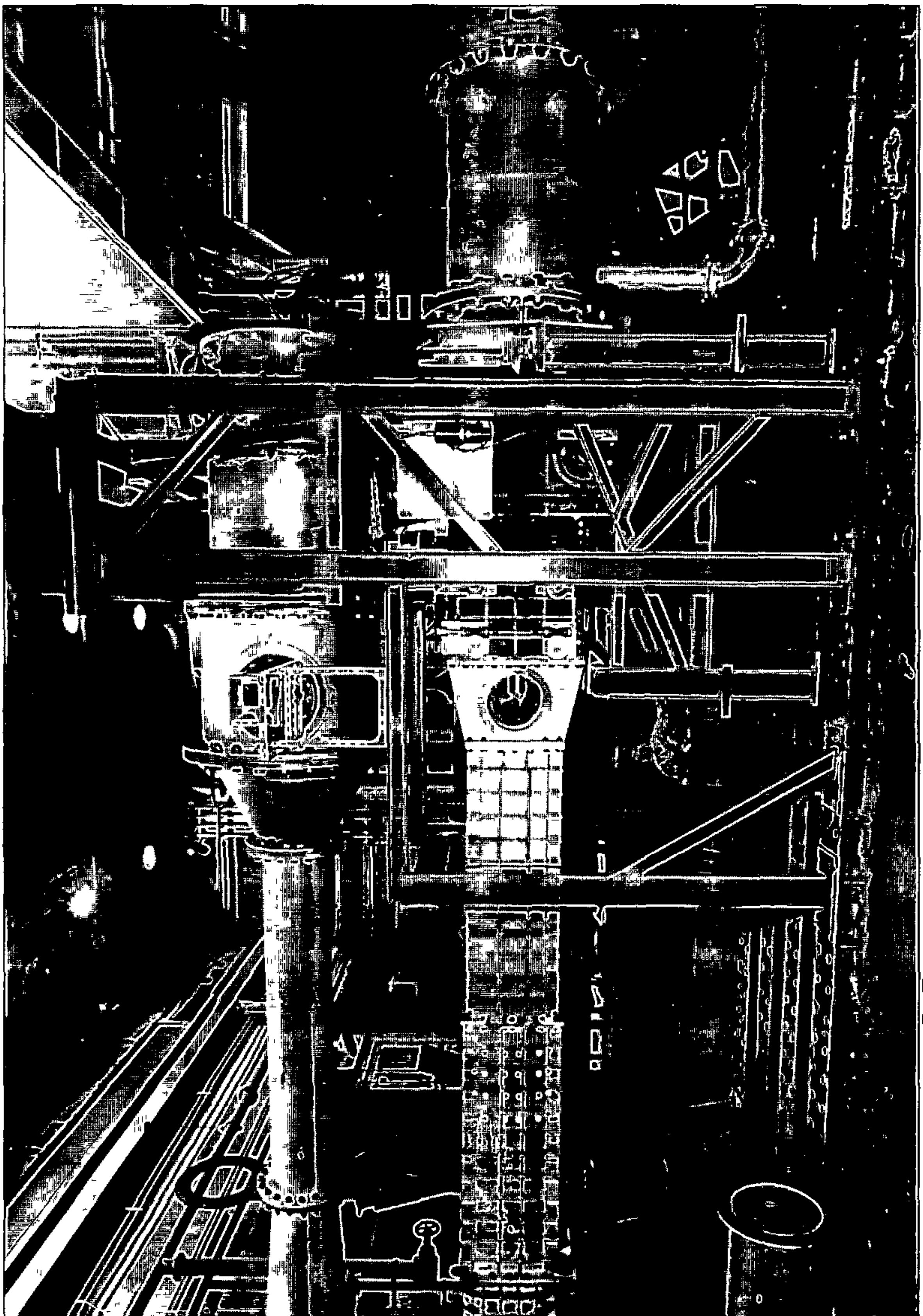

MODEL PROPELLING NOZZLE TEST RIG.

FIG. 2

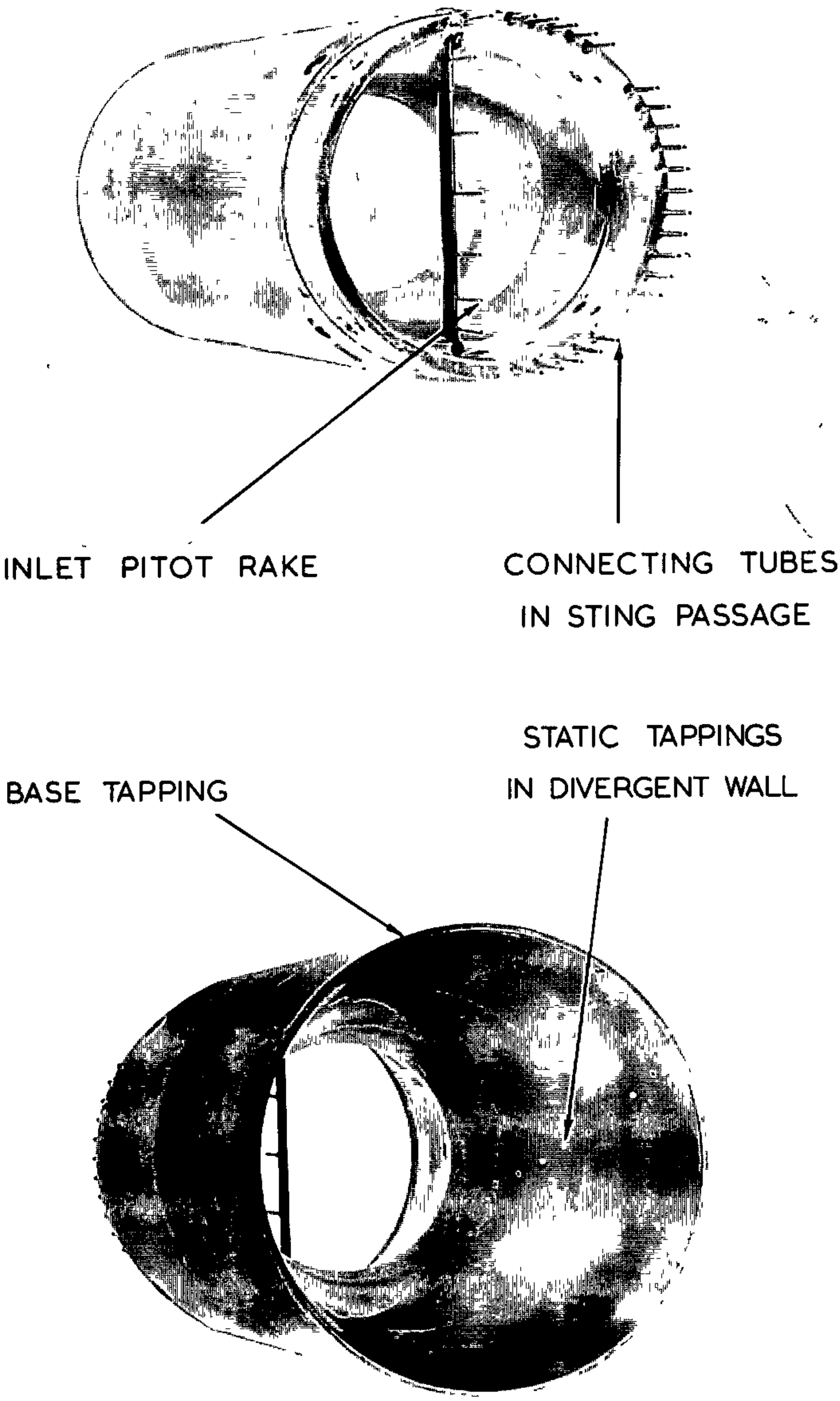

MODEL PROPELLING NOZZLE

FIG.3

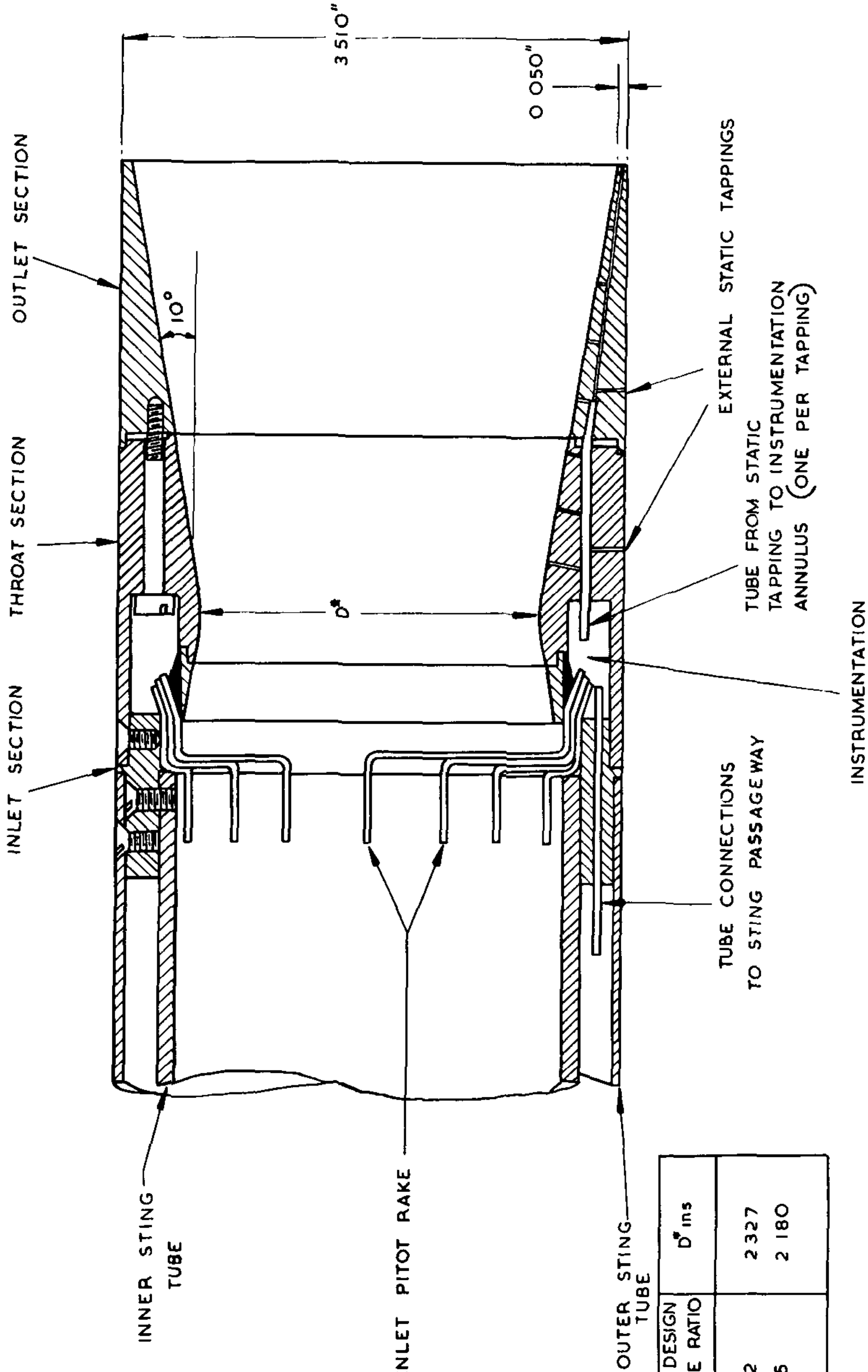

NOZZLE DESIGN PRESSURE RATIO	D* ins
12	2 327
15	2 180

INTERNAL ARRANGEMENT OF MODEL NOZZLE

FIG. 4

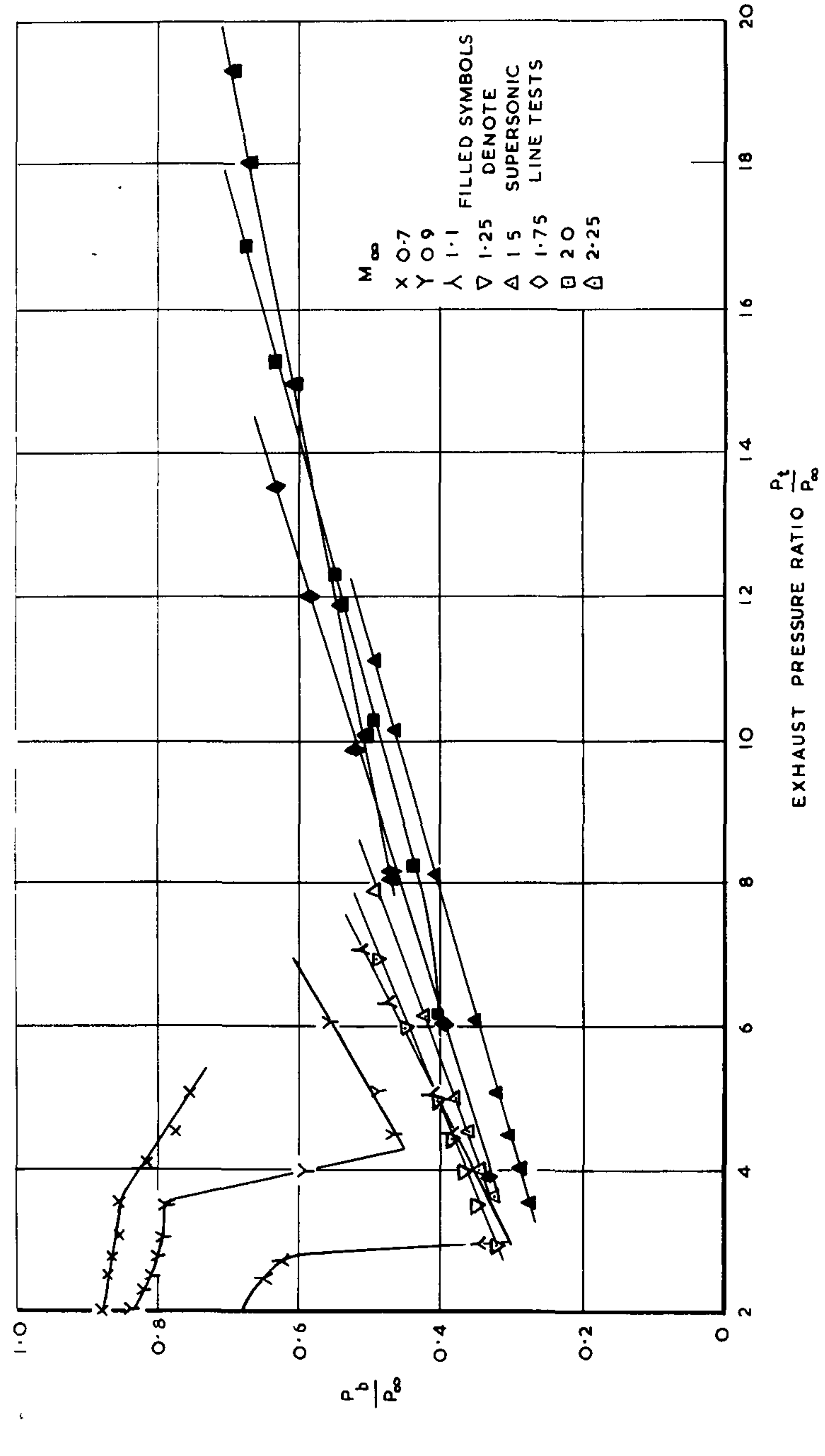

BASE PRESSURE RATIO — D.P.R. 15

BASE PRESSURE RATIO — D.P.R.12

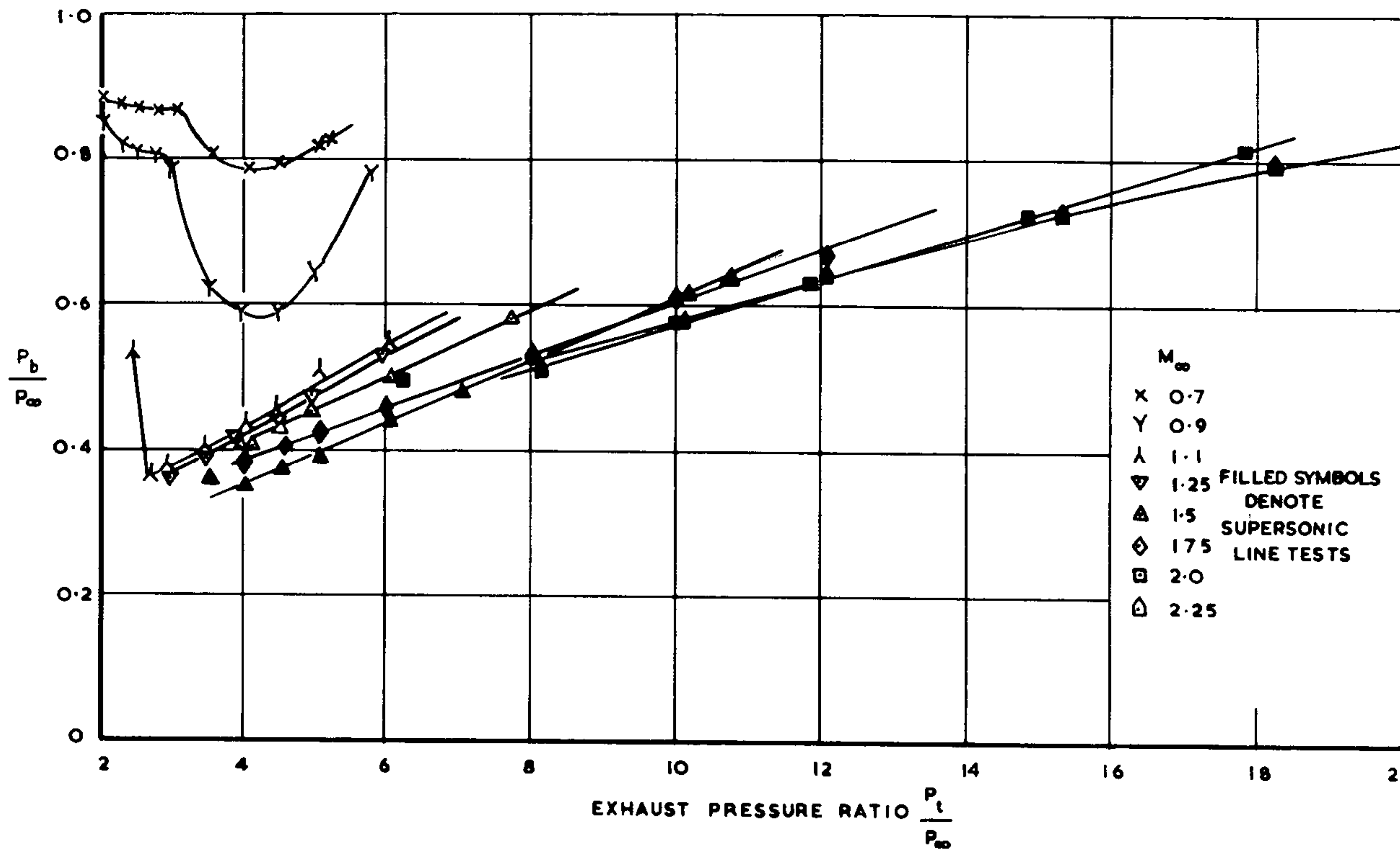

FIG.5

FIG. 6

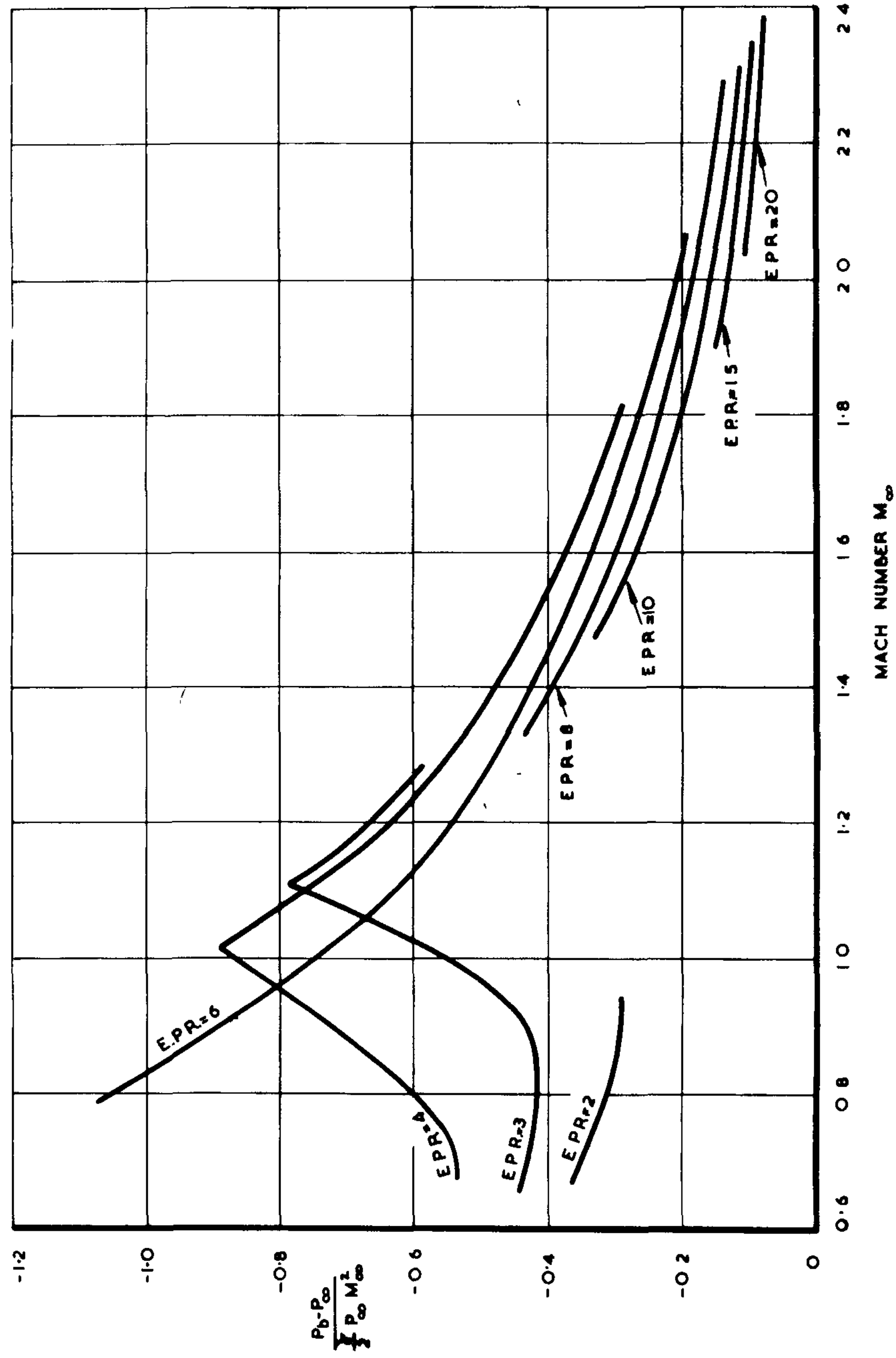

BASE PRESSURE COEFFICIENT – D.P.R. 15

FIG.7

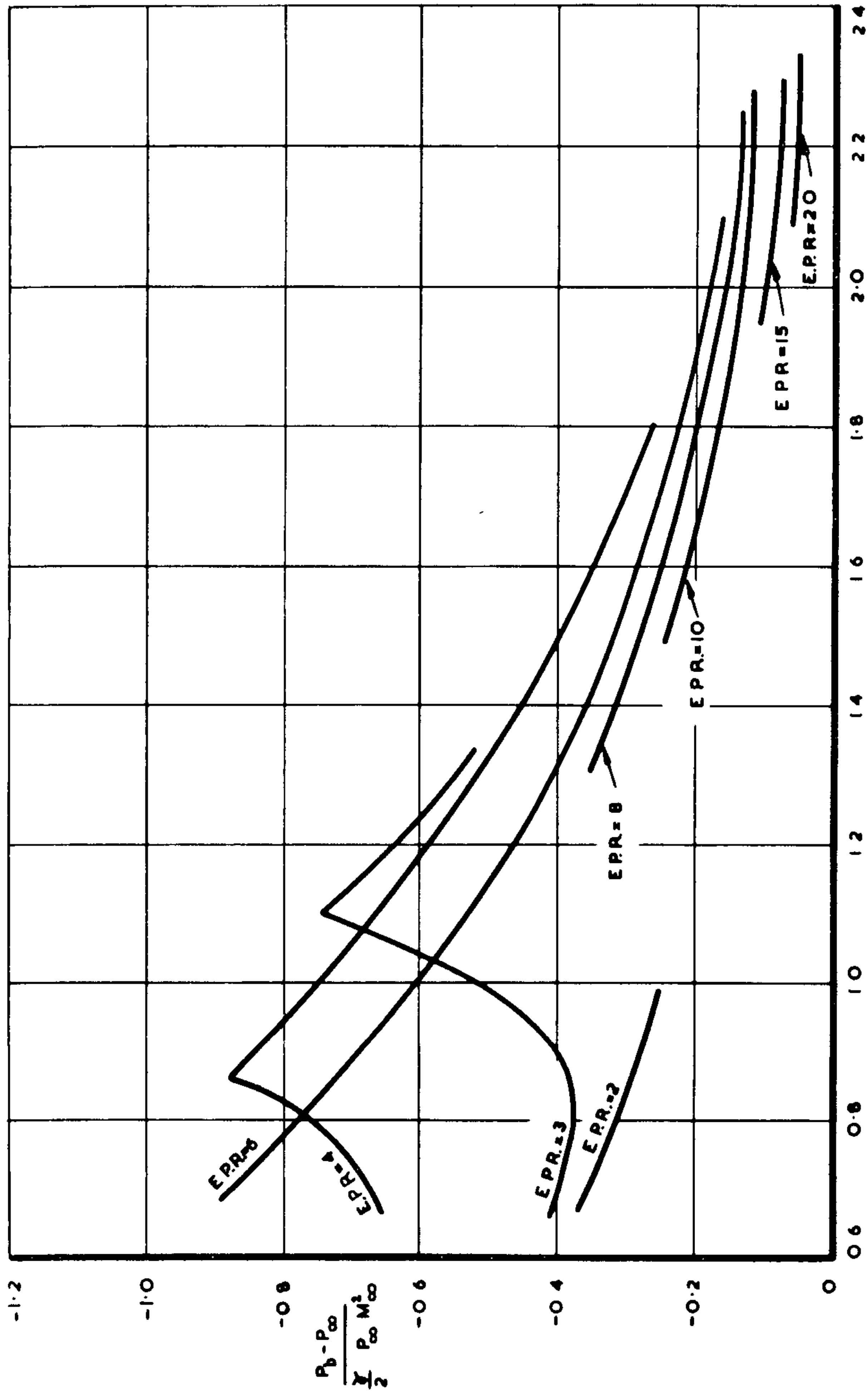

BASE PRESSURE COEFFICIENT–D.P.R.12

FIG. 8

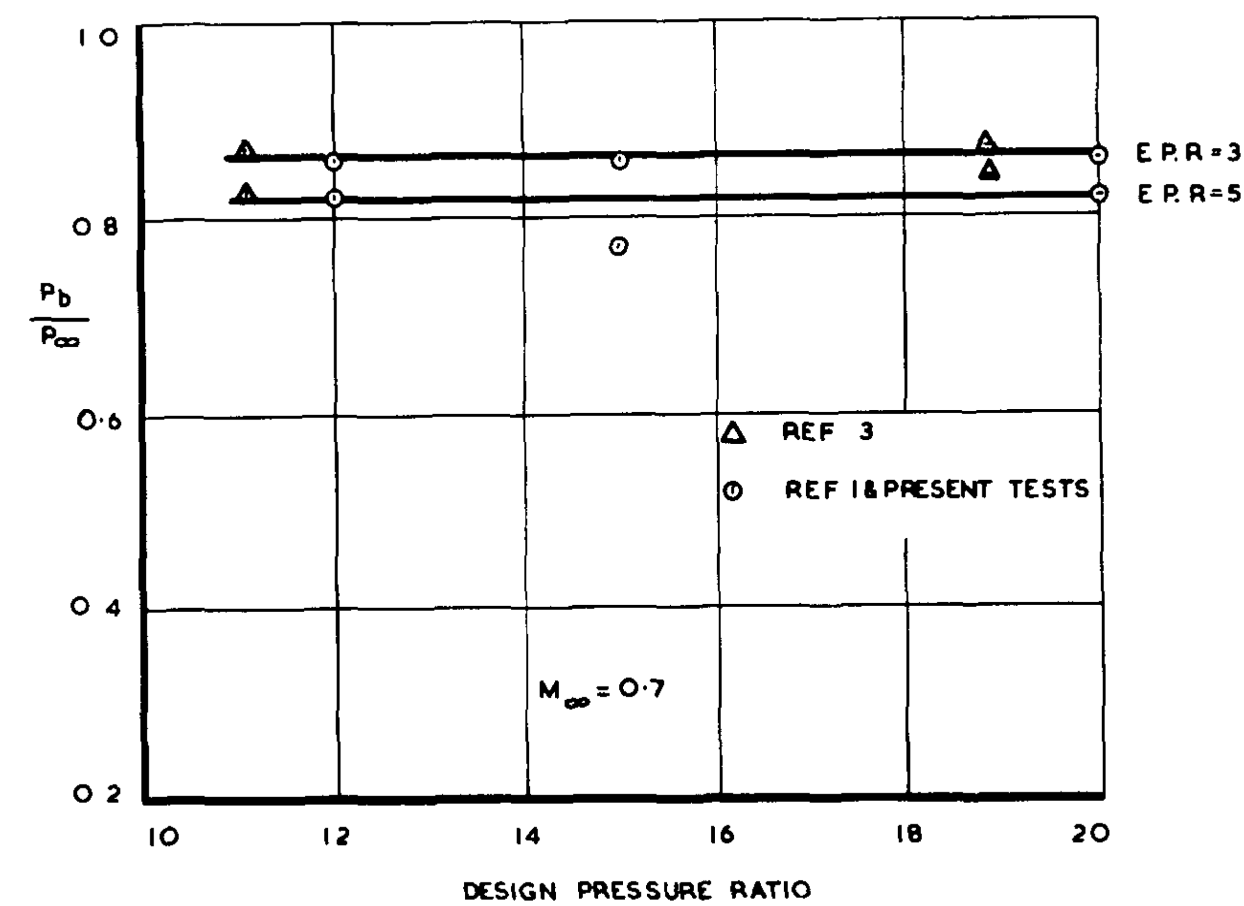

EFFECT OF D.P.R. ON BASE PRESSURE RATIO-I

FIG. 9

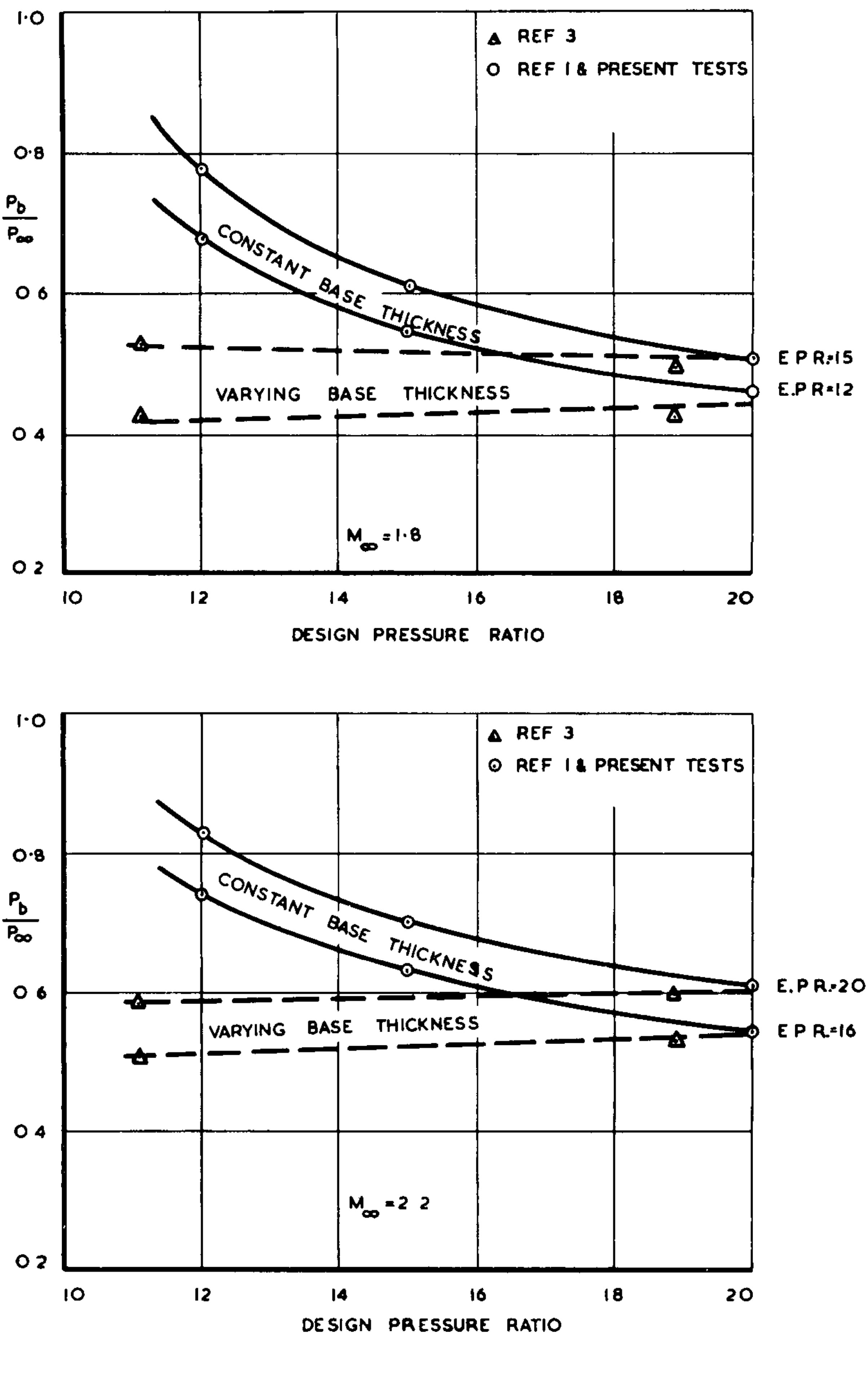

EFFECT OF D.P.R. ON BASE PRESSURE RATIO-II

FIG. 10

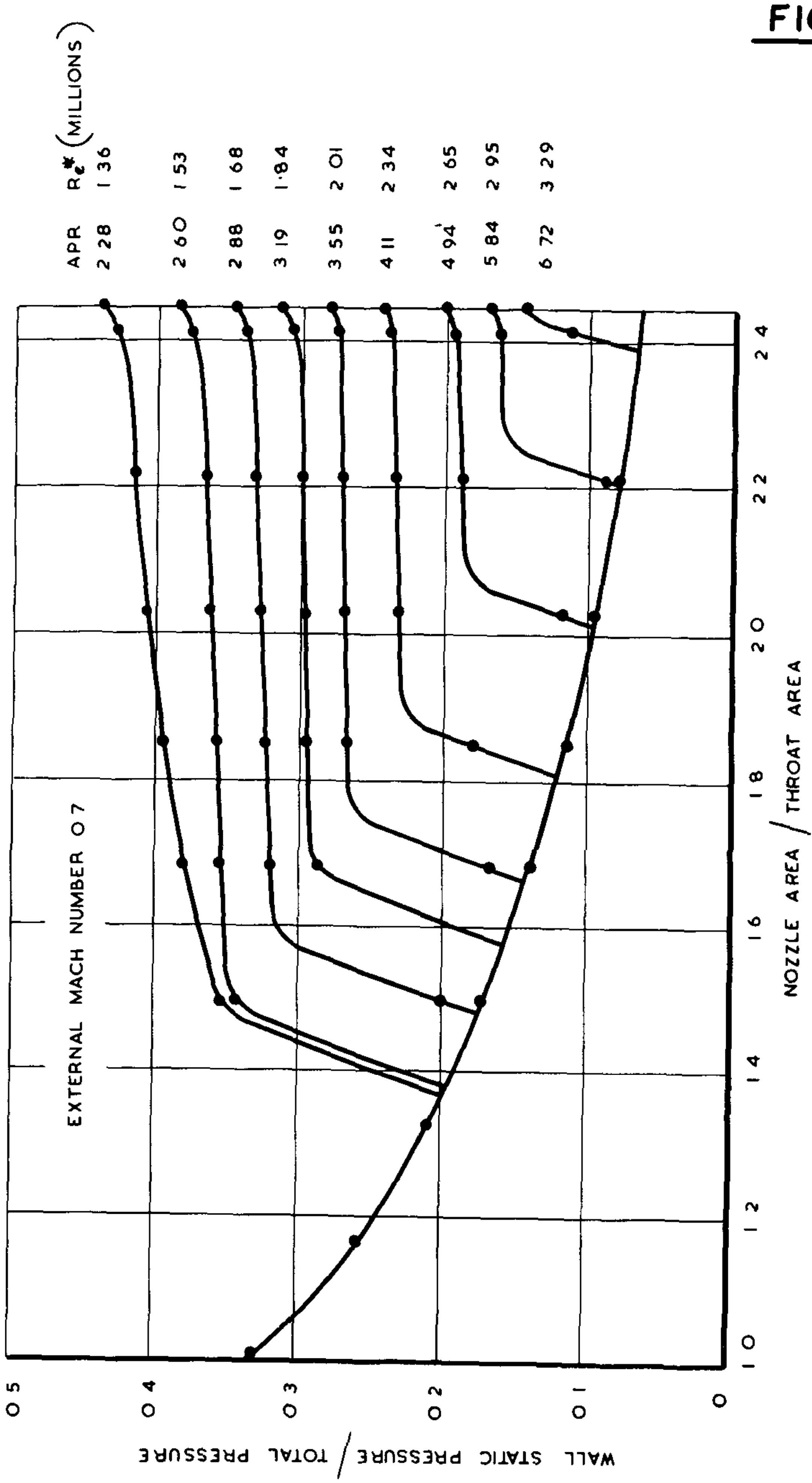

INTERNAL PRESSURE DISTRIBUTION – D.P.R. 15

FIG. 11

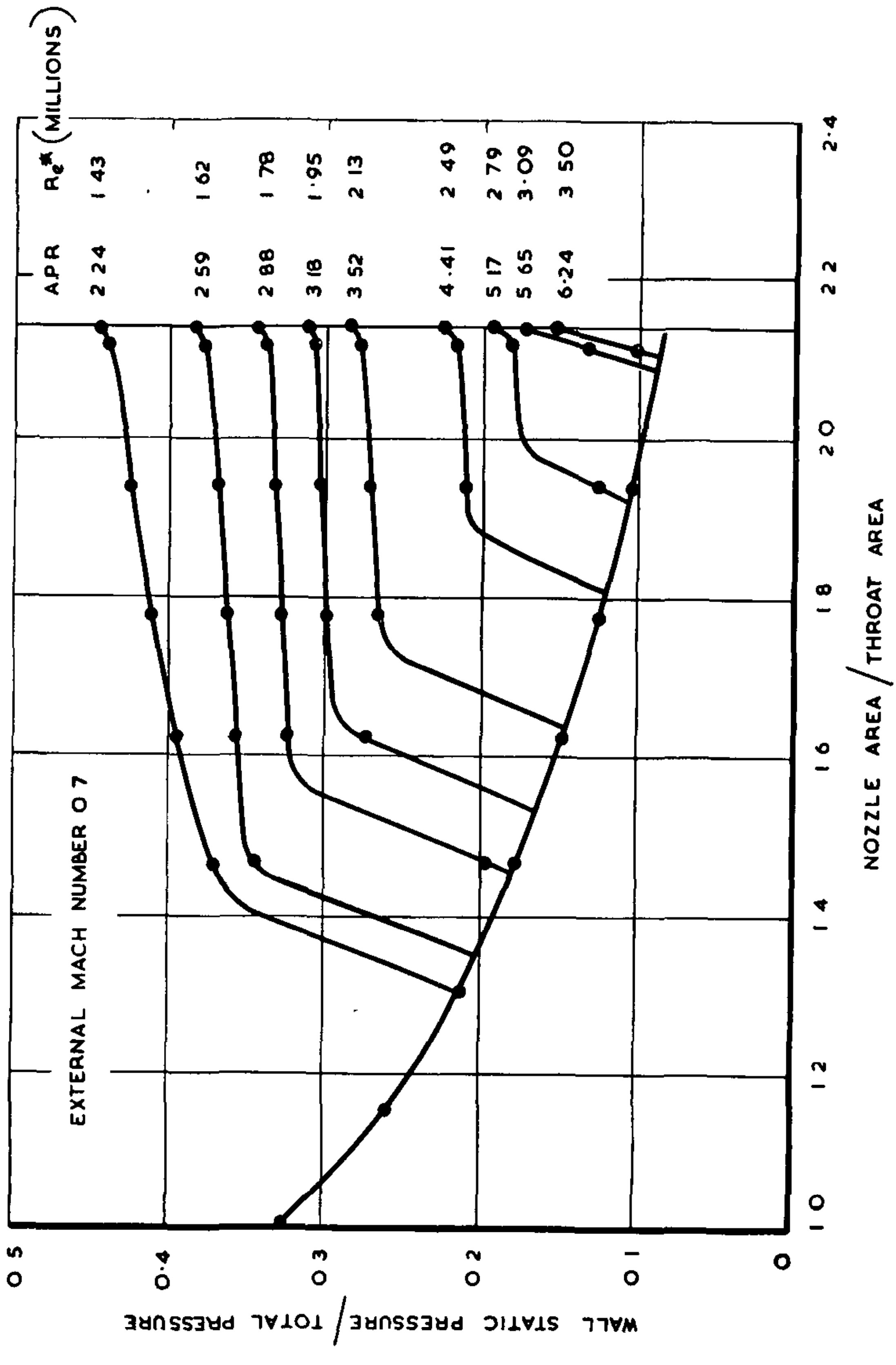

INTERNAL PRESSURE DISTRIBUTION–D.P.R. 12

EXTERNAL THRUST EFFICIENCY — D.P.R.15

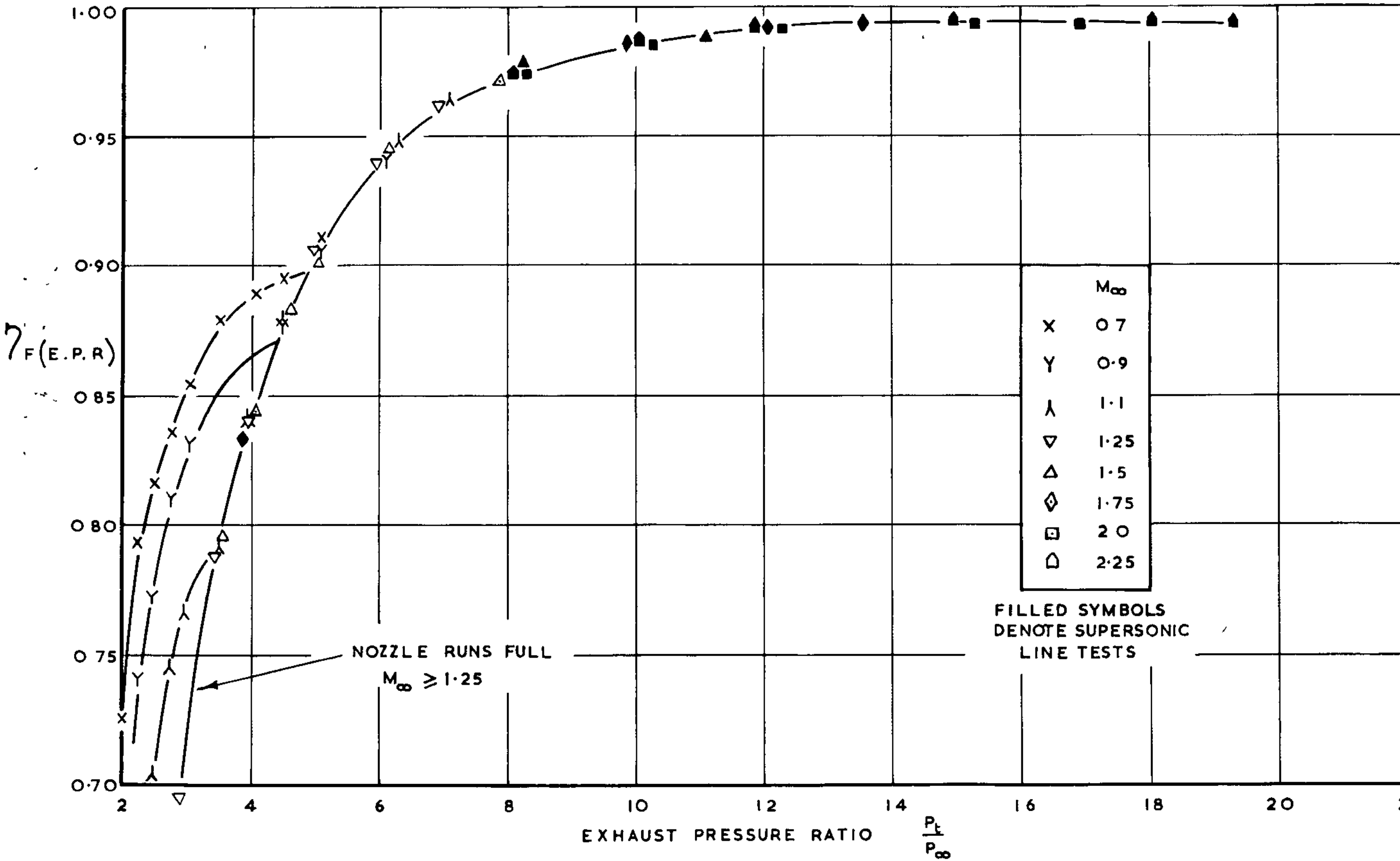

FIG.12

EXTERNAL THRUST EFFICIENCY — D.P.R.12

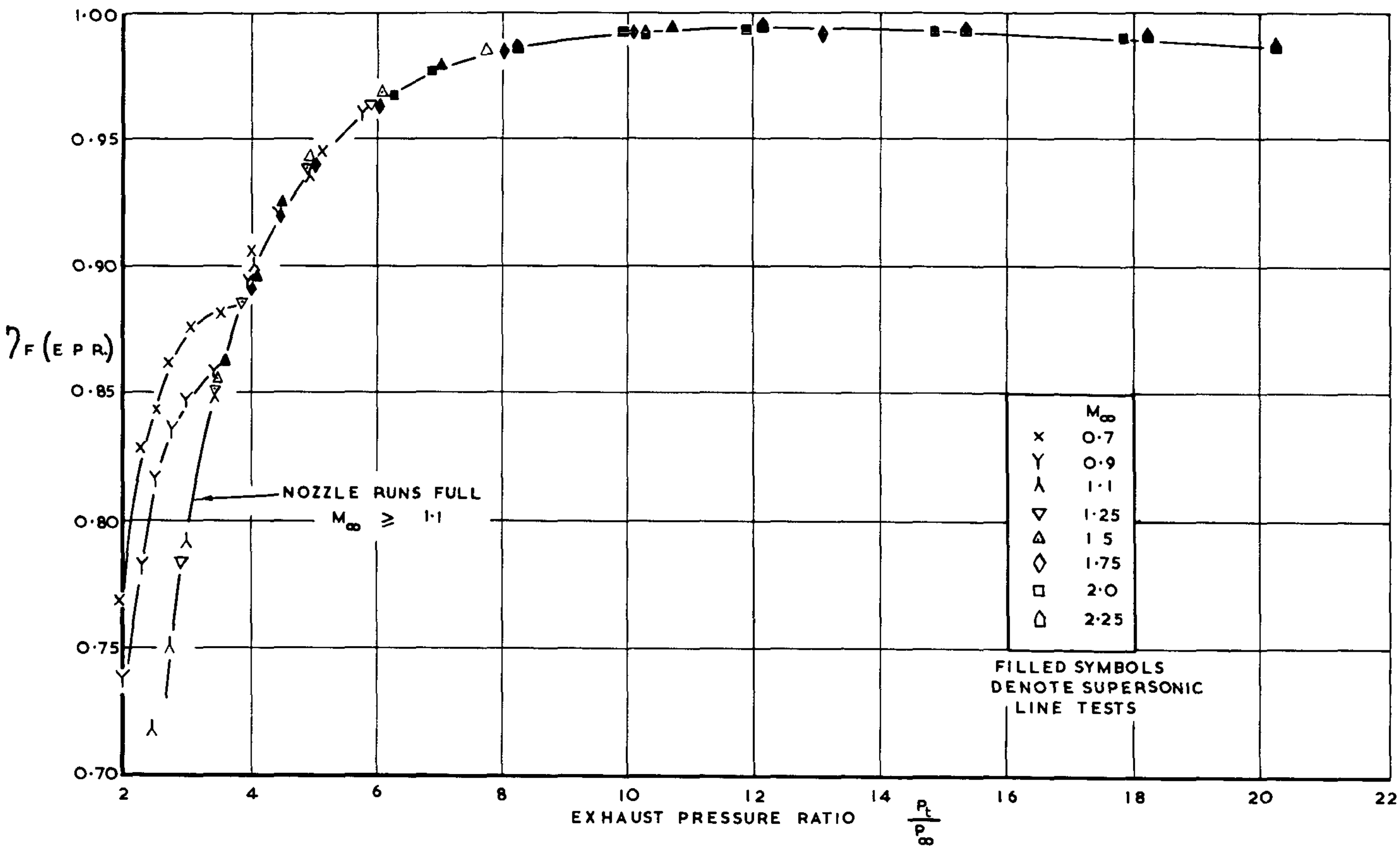

FIG.13

FIG.14

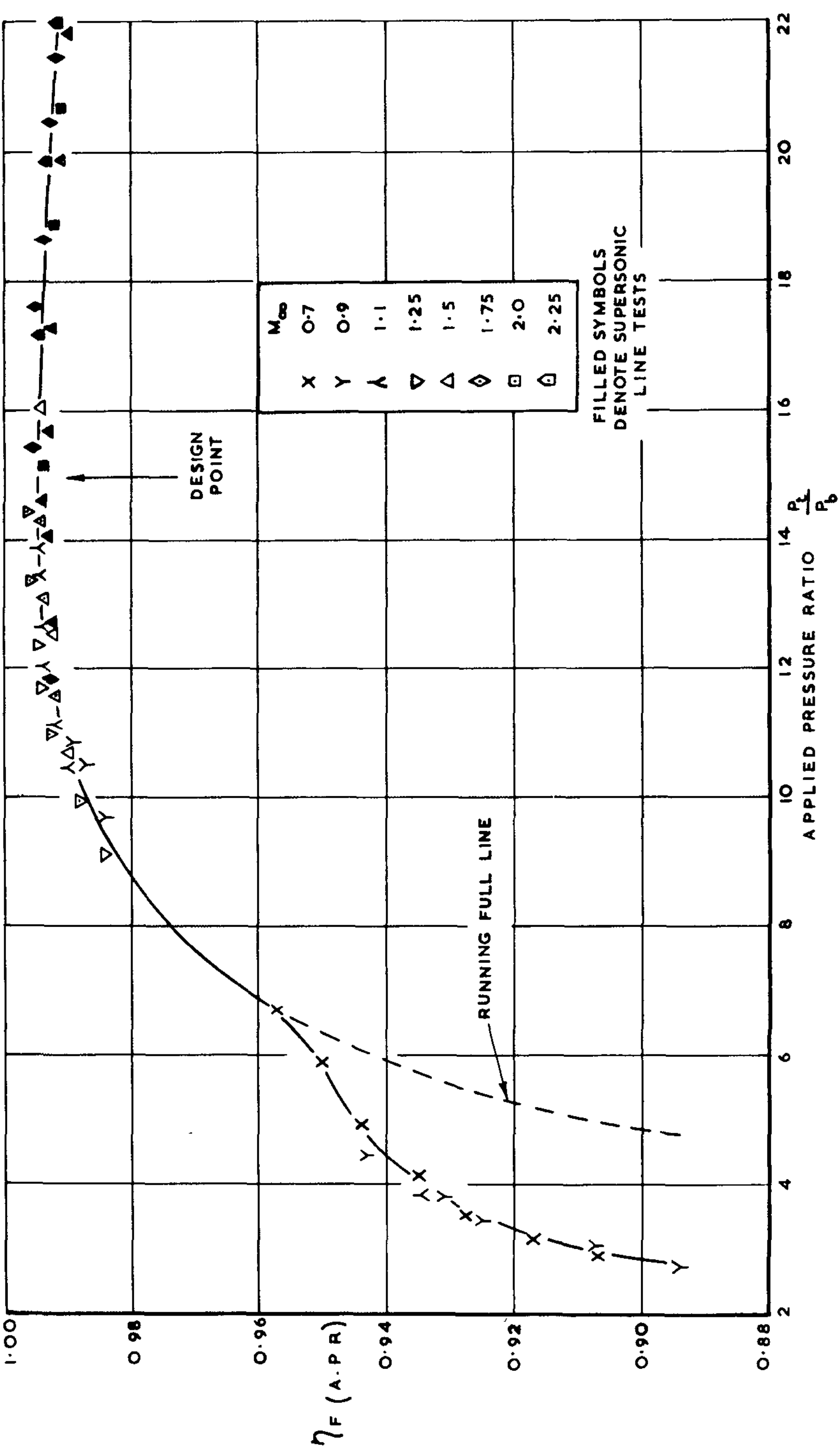

INTERNAL THRUST EFFICIENCY — D.P.R.15

FIG.15

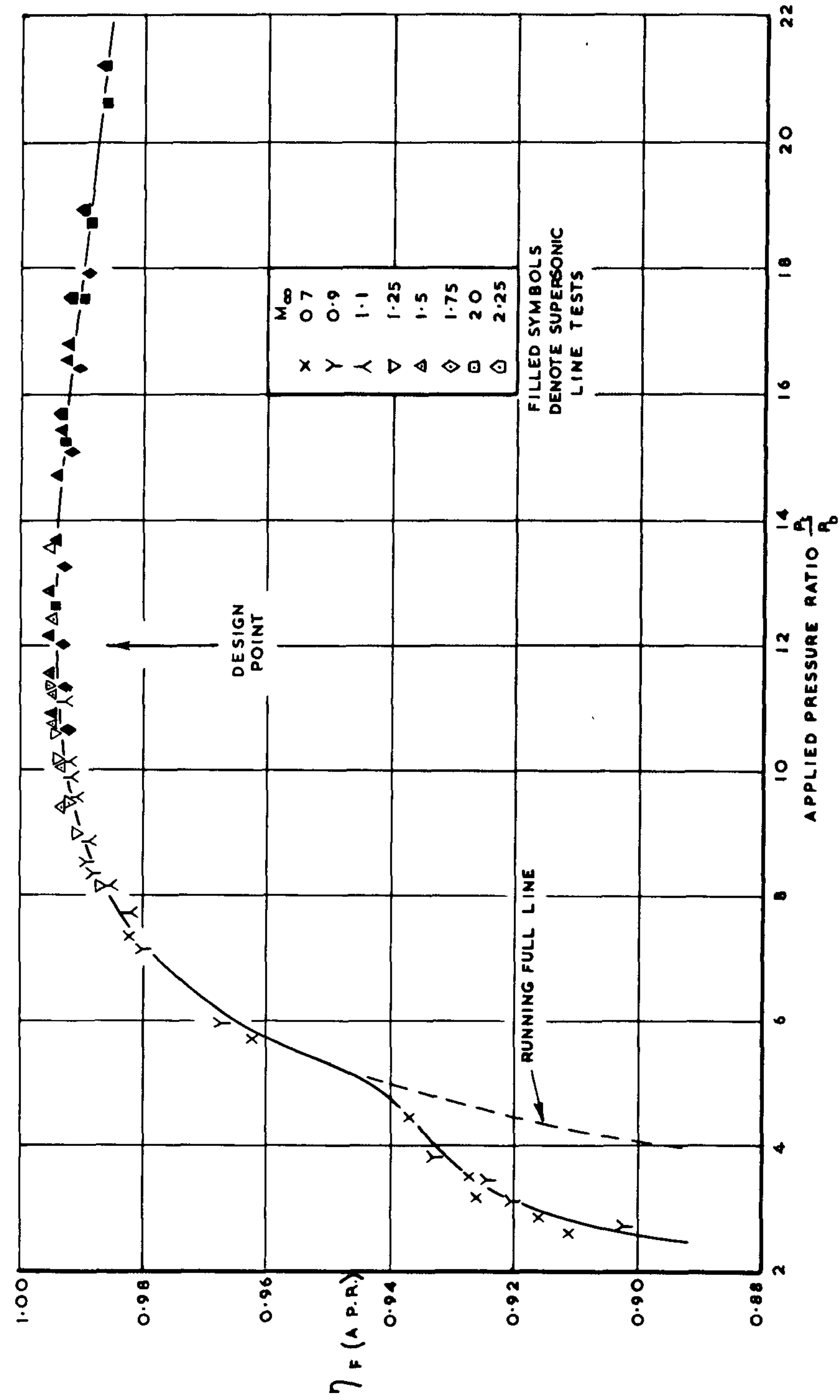

INTERNAL THRUST EFFICIENCY — D.P.R.12

FIG.16

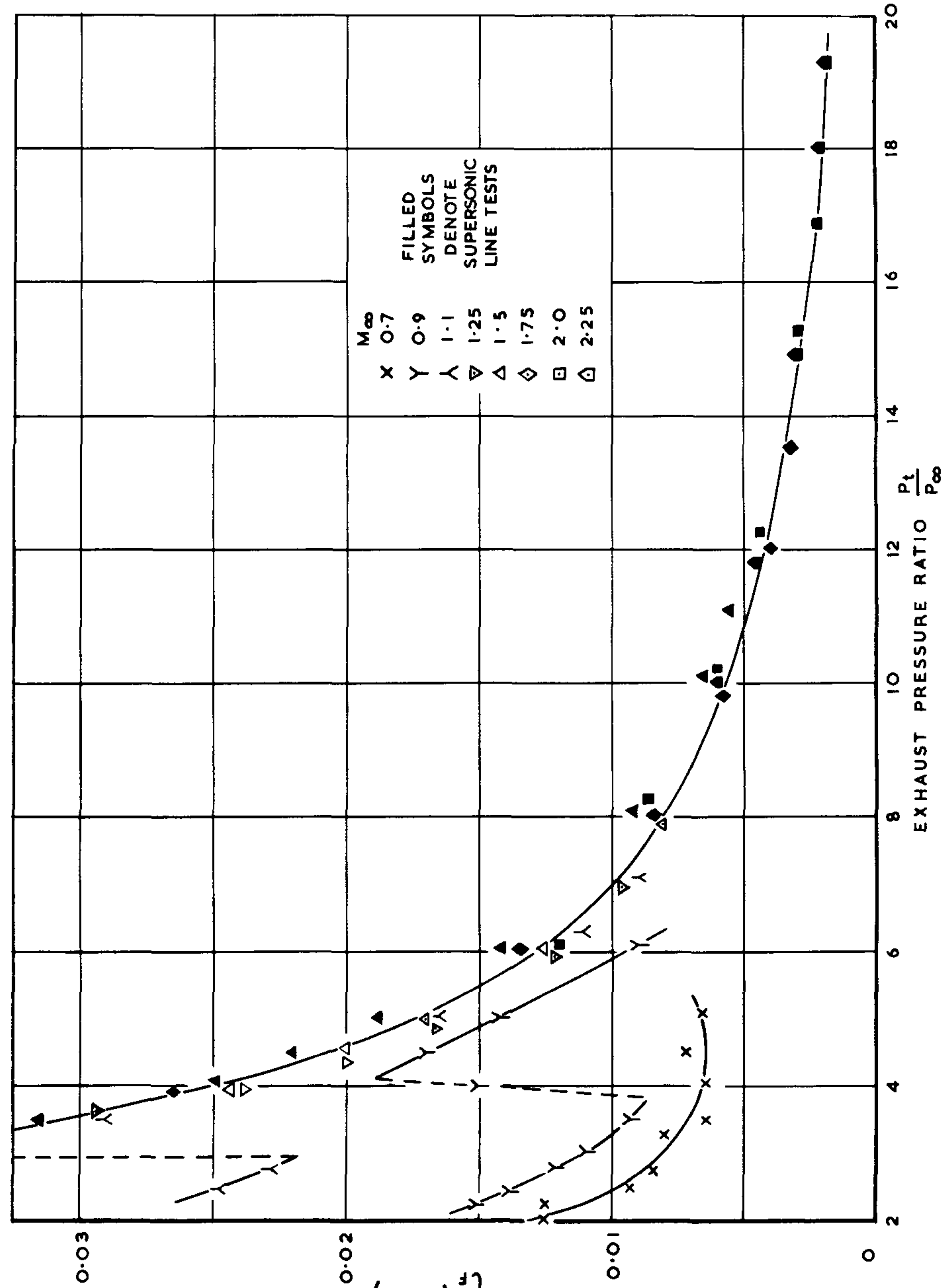

BASE DRAG TERM – D.P.R.15

BASE DRAG TERM — D.P.R.12

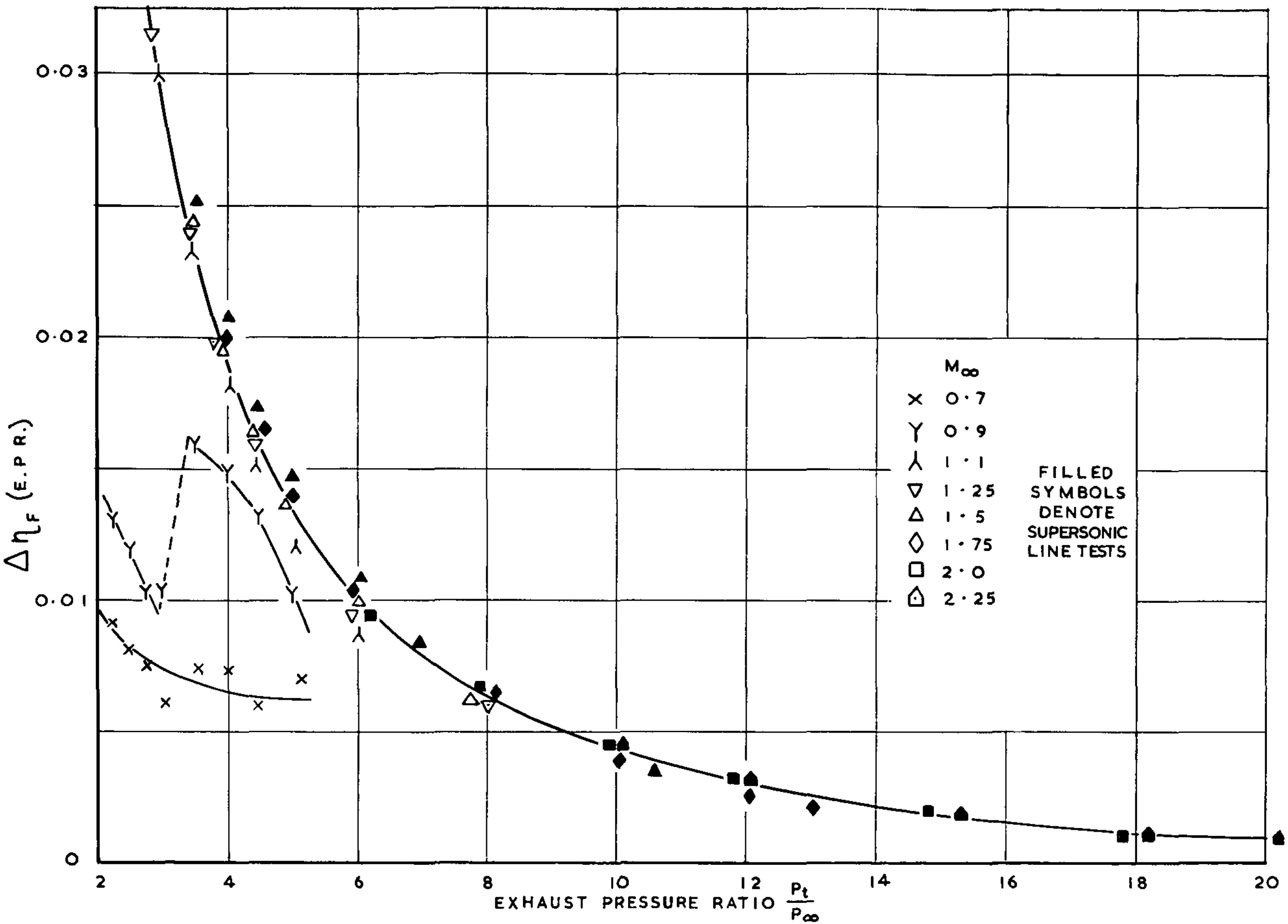

FIG.17

A.R.C. C.P. No.893 621-225.1:
February, 1964 533.691.18
Goleswothy, G. T., Roberts, J. B. and Overy, C.

THE PERFORMANCE OF CONICAL CONVERGENT-DIVERGENT NOZZLES OF AREA RATIOS 2.44 and 2.14 IN EXTERNAL FLOW

Two model internal-expansion propelling nozzles with conical divergence of 10° semi-angle, area ratios 2.44 and 2.14 (design pressure ratios 15 and 12), parallel afterbodies and thin annular bases, have been tested in external flow over the range of Mach No. 0.7 to 2.25. Measurements have been made of nozzle base pressure, and thrust efficiencies derived with reference to both ambient and base pressure levels.

It is found that, in supersonic external flow, with complete expansion of nozzle internal flow to ambient pressure, the value of base pressure ratio is independent of nozzle design pressure ratio, provided the base thickness is unchanged. For a given overall operating pressure ratio,

P.T.O.

A.R.C. C.P. No.893 621-225.1:
February, 1964 533.691.18
Goleswothy, G. T., Roberts, J. B. and Overy, C.

THE PERFORMANCE OF CONICAL CONVERGENT-DIVERGENT NOZZLES OF AREA RATIOS 2.44 and 2.14 IN EXTERNAL FLOW

Two model internal-expansion propelling nozzles with conical divergence of 10° semi-angle, area ratios 2.44 and 2.14 (design pressure ratios 15 and 12), parallel afterbodies and thin annular bases, have been tested in external flow over the range of Mach No. 0.7 to 2.25. Measurements have been made of nozzle base pressure, and thrust efficiencies derived with reference to both ambient and base pressure levels.

It is found that, in supersonic external flow, with complete expansion of nozzle internal flow to ambient pressure, the value of base pressure ratio is independent of nozzle design pressure ratio, provided the base thickness is unchanged. For a given overall operating pressure ratio,

P.T.O.

A.R.C. C.P. No.893 621-225.1:
February, 1964 533.691.18
Goleswothy, G. T., Roberts, J. B. and Overy, C.

THE PERFORMANCE OF CONICAL CONVERGENT-DIVERGENT NOZZLES OF AREA RATIOS 2.44 and 2.14 IN EXTERNAL FLOW

Two model internal-expansion propelling nozzles with conical divergence of 10° semi-angle, area ratios 2.44 and 2.14 (design pressure ratios 15 and 12), parallel afterbodies and thin annular bases, have been tested in external flow over the range of Mach No. 0.7 to 2.25. Measurements have been made of nozzle base pressure, and thrust efficiencies derived with reference to both ambient and base pressure levels.

It is found that, in supersonic external flow, with complete expansion of nozzle internal flow to ambient pressure, the value of base pressure ratio is independent of nozzle design pressure ratio, provided the base thickness is unchanged. For a given overall operating pressure ratio,

P.T.O.

DETACHABLE ABSTRACT CARDS

again with constant base thickness, the effect of decreasing nozzle design pressure ratio is to raise base pressure ratio. In subsonic external flow, for a given overall operating pressure ratio, base pressure ratio can be independent of nozzle design pressure ratio.

again with constant base thickness, the effect of decreasing nozzle design pressure ratio is to raise base pressure ratio. In subsonic external flow, for a given overall operating pressure ratio, base pressure ratio can be independent of nozzle design pressure ratio.

again with constant base thickness, the effect of decreasing nozzle design pressure ratio is to raise base pressure ratio. In subsonic external flow, for a given overall operating pressure ratio, base pressure ratio can be independent of nozzle design pressure ratio.

C.P. No. 893

Printed and published by
HER MAJESTY'S STATIONERY OFFICE
To be purchased from
49 High Holborn, London W C 1
423 Oxford Street, London W 1
13A Castle Street, Edinburgh 2
109 St Mary Street, Cardiff
Brazennose Street, Manchester 2
50 Fairfax Street, Bristol 1
35 Smallbrook, Ringway, Birmingham 5
80 Chichester Street, Belfast 1
or through any bookseller

Printed in England

C.P. No. 893

S.O. Code No 23-9016-93